

## Multiple Roles of Protein Kinase A in Arachidonic Acid-Mediated $\text{Ca}^{2+}$ Entry and Tumor-Derived Human Endothelial Cell Migration

Alessandra Fiorio Pla<sup>1,2,3</sup>, Tullio Genova<sup>1</sup>, Emanuela Pupo<sup>1</sup>, Cristiana Tomatis<sup>1,2,3</sup>, Armando Genazzani<sup>4</sup>, Roberta Zaninetti<sup>4</sup>, and Luca Munaron<sup>1,2,3</sup>

### Abstract

We recently showed that arachidonic acid (AA) triggers calcium signals in endothelial cells derived from human breast carcinoma (B-TEC). In particular, AA-dependent  $\text{Ca}^{2+}$  entry is involved in the early steps of tumor angiogenesis *in vitro*. Here, we investigated the multiple roles of the nitric oxide (NO) and cyclic AMP/protein kinase A (PKA) pathways in AA-mediated  $\text{Ca}^{2+}$  signaling in the same cells. B-TEC stimulation with 5  $\mu\text{mol/L}$  AA resulted in endothelial NO synthase (NOS) phosphorylation at Ser<sup>1177</sup>, and NO release was measured with the fluorescent NO-sensitive probe DAR4M-AM. PKA inhibition by the use of the membrane-permeable PKA inhibitory peptide myristoylated PKI<sub>14-22</sub> completely prevented both AA- and NO-induced calcium entry and abolished B-TEC migration promoted by AA. AA-dependent calcium entry and cell migration were significantly affected by both the NOS inhibitor *N*<sup>G</sup>-nitro-L-arginine methyl ester and the NO scavenger 2-phenyl-4,4,5,5-tetramethylimidazole-1-oxyl 3-oxide, suggesting that NO release is functionally involved in the signaling dependent on AA. Moreover, pretreatment with carboxyamidotriazole, an antiangiogenic compound that interferes with agonist-activated calcium entry, prevented AA-dependent B-TEC motility. Interestingly, even in the absence of AA, enhancement of the cyclic AMP/PKA pathway with the adenylyl cyclase activator forskolin evoked a calcium entry dependent on NOS recruitment and NO release. The functional relevance of AA-induced calcium entry could be restricted to tumor-derived endothelial cells (EC) because AA evoked a smaller calcium entry in normal human microvascular ECs compared with B-TECs, and even more importantly, it was unable to promote cell motility in wound healing assay. This evidence opens an intriguing opportunity for differential pharmacologic treatment between normal and tumor-derived human ECs. *Mol Cancer Res*; 8(11); 1466–76. ©2010 AACR.

### Introduction

Angiogenic growth factors, such as basic fibroblast growth factor and vascular endothelial growth factor (VEGF), trigger a signaling cascade involving activation of specific tyrosine kinase receptors and recruitment of cell effectors, including PLC- $\gamma$ , endothelial nitric oxide synthase (eNOS), and PLA<sub>2</sub>, leading to the production of IP<sub>3</sub>, nitric oxide (NO), arachidonic acid (AA), and their metabolites (1, 2). These pathways promote store-operated and non-store-operated  $\text{Ca}^{2+}$  entry (SOCE and NSOCE,

respectively) from extracellular medium into endothelial cells (EC; refs. 3, 4).

In particular, we previously reported the ability of AA to trigger a NSOCE in bovine aortic ECs (BAEC), playing a critical role in the control of proliferation (1, 2, 5-7).

Because blood vessels in tumors differ from normal ones by their altered morphology, blood flow, permeability, and abnormalities in pericytes and in basement membrane, several groups have recently focused their attention on tumor-derived ECs (TEC) as a more adequate model to study tumor angiogenesis (8). Interestingly, TECs display a distinct and unique phenotype different from that of normal vascular ECs at molecular and functional levels (9-11). Recently, TECs obtained from breast carcinomas (B-TEC) have been established and characterized, showing an immature proangiogenic phenotype with enhanced proliferation, motility, and capillary-like tube formation compared with “normal” ECs (10, 12). Therefore, they represent an interesting model to investigate the role of different factors in the tumoral angiogenic process.

We have recently studied the role of AA-induced cytosolic calcium ( $\text{Ca}_c$ ) signals in the angiogenic process of

**Authors' Affiliations:** <sup>1</sup>Department of Animal and Human Biology, <sup>2</sup>Nanostructured Interfaces and Surfaces Centre of Excellence (NIS), and <sup>3</sup>Center for Complex Systems in Molecular Biology and Medicine (SysBioM), University of Turin, Turin, Italy; and <sup>4</sup>DISCAFF, University of Piemonte Orientale, Novara, Italy

**Corresponding Author:** Luca Munaron, Department of Animal and Human Biology, University of Turin, Via Accademia Albertina 13, 10123 Turin, Italy. Phone: 39-011-6704667; Fax: 39-011-6704508. E-mail: luca.munaron@unito.it

doi: 10.1158/1541-7786.MCR-10-0002

©2010 American Association for Cancer Research.

B-TECs (5). AA induces B-TEC proliferation and increases capillary-like formation *in vitro*. Notably, calcium entry promoted by the fatty acid is specifically detected in the early stages of tubule organization and downregulated in the later phases of capillary-like organization. The use of the antiangiogenic agent carboxyamidotriazole (CAI) reduces AA-induced  $Ca_c$  signals and completely prevents AA-induced *in vitro* tubulogenesis (5).

It is well known that NO release, produced by NO synthases (NOS), mediates angiogenesis (13, 14). NO exposure increases DNA synthesis, proliferation, and migration of ECs. NO mediates the function of many angiogenic factors and interferes with their expression. Furthermore, NO, through cyclic guanosine 3',5'-monophosphate (cGMP)-dependent and cGMP-independent pathways, is able to regulate different types of calcium-permeable channels in ECs (1, 2, 4, 13-20). In this context, we previously reported a crosstalk between arachidonate-activated calcium signals and NO metabolism (6). Both AA and NO actually induce a NSOCE in BAECs (1, 2, 5-7); in the same cells, AA promotes NO release even in the absence of calcium entry, giving rise to a complex signaling pathway for NSOCE regulation (6).

Here, we tested the modulation of AA-dependent calcium entry by NO in B-TECs, focusing our attention on the role of the cyclic AMP (cAMP)/protein kinase A (PKA) pathway. PKA regulates eNOS activity through serine phosphorylation, and it has been recently reported that forskolin, a widely used adenylyl cyclase activator, is able to trigger proangiogenic effects through the PI3K, Akt, and eNOS pathways in human umbilical vascular ECs (21, 22). In addition, it is worth noting that a number of different endothelial calcium-permeable channels are substrates for PKA phosphorylation, including some members of the transient receptor potential (TRP) superfamily of proteins. Interestingly, some of them (including TRPV1 and TRPV4) are also regulated by AA and its metabolites, as well as by NO through S-nitrosylation (23-26).

## Materials and Methods

### Cell cultures

Tumor-derived ECs were obtained from breast lobular-infiltrating carcinoma (B-TEC). ECs were isolated, using anti-CD105 antibody coupled to magnetic beads, by magnetic cell sorting using the MACS system (Miltenyi Biotec) and grown in complete EBM (Cambrex) supplemented with 10% FCS (Cambrex), 50  $\mu$ g/mL gentamicin (Cambrex), and 2 mmol/L glutamine (Cambrex) as previously described (10). Cells were used at passages 3 to 15. Moreover, periodically, cells were characterized by the morphology and expression of a panel of endothelial antigens such as CD105, CD31, Muc-18 (CD146), CD44, and VEGF receptor 2 (KDR; ref. 10). Adult human dermal microvascular ECs (HMEC) were purchased from Lonza and grown in EGM 2-MV medium (Lonza).

### Materials

Calcium and NO probes (fura-2-AM and DAR4M-AM) were purchased from Molecular Probes, Inc. Unless otherwise specified, all other reagents were obtained from Sigma.

### Calcium imaging

For ratiometric  $Ca_c$  measurements, cells were loaded with the acetoxymethyl ester form of fura-2 (2.5  $\mu$ mol/L fura-2-AM, 45 minutes at 37°C) and imaged at 0.8-second intervals using a monochromator system attached to a TE-2000 Nikon inverted microscope with a Fluor 20 $\times$  objective. Images were acquired using an enhanced charge-coupled device camera and Metafluor software (Universal Imaging Corporation; Crisel Instruments).

B-TECs were seeded on glass gelatin-coated coverslips at a density of 5,000 cells/cm<sup>2</sup> in DMEM containing 5% FCS 1 to 2 days before the experiments.

During the experiments, B-TECs were maintained in standard Tyrode solution of the following composition (in mmol/L): NaCl, 154; KCl, 4; CaCl<sub>2</sub>, 2; MgCl<sub>2</sub>, 1; HEPES, 5; glucose, 5.5; NaOH to pH 7.35. Cells were continuously bathed with a microperfusion system (inner pipette diameter, 250  $\mu$ m); for experiments in calcium-free conditions, the external solution was modified by omitting the CaCl<sub>2</sub> salt from the formulation and adding the calcium chelator EGTA (5 mmol/L).  $\Delta R$  is a measure of calcium response amplitude and is calculated as the difference between R at the peak of the response and R before agonist application.

### NO measurements

Cells were loaded with DAR4M-AM (5  $\mu$ mol/L, 30 minutes at 37°C) and excited at 568 nm. Emission signals were filtered by 610-nm band pass filters and detected with the scanning head.

Confocal fluorimetric measurements were done using an Olympus Fluoview 200 laser scanning confocal system (Olympus America, Inc.) mounted on an inverted IX70 Olympus microscope, equipped with a 60 $\times$  oil-immersion objective (numerical aperture, 0.17). X-Y plane images (resolution, 800  $\times$  600 pixels) were acquired every 1.6 seconds and stored in the multi TIFF file format.

### Wound healing assays

Cell motility was investigated as migration of cells into a wound introduced in a confluent monolayer. B-TECs were grown to confluence on 12-well culture plates coated with 1% gelatin. Cell monolayers were allowed to rest for 12 hours in DMEM containing 2% FCS, and a "wound" was made under standard conditions by scraping the middle of the cell monolayer with a P10 pipette tip. Floating cells were removed by washing with PBS, and the cell monolayer was treated with test conditions (see Results). Cells did not undergo any significant degree of cell division during the experiments. Experiments were done using a Nikon T-E microscope with a 4 $\times$  objective. Cells were kept at 37°C and 5% CO<sub>2</sub> for all experiments; a photo was taken every 2 hours using Metamorph software. Cell motility

into a wound was measured with ImageJ software and was expressed as percentage of cell migration. At least three fields for each condition were analyzed in each independent experiment. At least three independent experiments were done for each experimental condition.

### Microchemotaxis assay

The assay was done using a 48-well Boyden's microchemotaxis chamber according to the manufacturer's instruction (Neuro Probe). Briefly, cells grown in complete EBM to subconfluence were suspended ( $2 \times 10^5$  cells/50  $\mu$ L) in serum-free DMEM containing 0.25% bovine serum albumin and placed in the open-bottom wells of the upper compartment of Boyden's chamber. The lower compartment of the chamber was loaded with 10 nmol/L oxytocin, 100 ng/mL VEGF, 5  $\mu$ mol/L AA, or control medium. Each pair of wells was separated by a polyvinylpyrrolidone-free polycarbonate porous membrane (8- $\mu$ m pores) precoated with gelatin (0.2 mg/mL in PBS). The chamber was then kept overnight in the cell culture incubator. At the end of the incubation period, the cells that migrated through the pores and adhered to the underside of the membrane were fixed and stained with the Diff-Quick kit (Biomap) and then mounted onto glass slides. Chemokinesis (the stimulation of increased random cell motility) was distinguished from chemotaxis by placing the same concentration of AA in both the upper and lower wells of the chamber, thereby eliminating the chemical gradient.

For quantitative analysis, the membranes were observed under a Nikon microscope using a 20 $\times$  objective. Five random fields of stained cells were counted for each well, and the mean number of migrating cells was calculated. Numbers in the text and figures are expressed as percent of control for clarity.

### Protein extraction and Western blot analysis

B-TECs were grown in EBM containing 10% FCS until 80% confluent. Cells were detached and suspended in ice-cold PBS containing the following protease inhibitors: 2  $\mu$ g/mL aprotinin, 1 mmol/L Na orthovanadate, 0.1 mmol/L phenylmethylsulfonyl fluoride, and 10 mmol/L

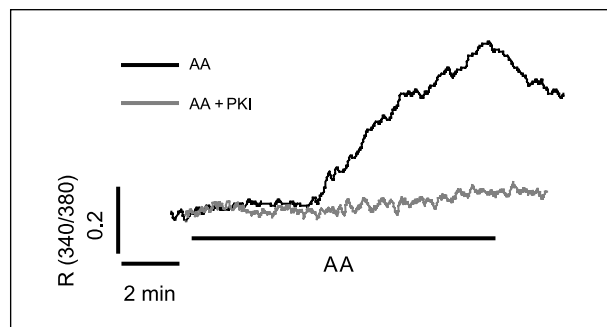


**FIGURE 1.** Effects of cAMP/PKA on AA-induced calcium entry in B-TECs. Representative traces showing  $Ca_c$  signals activated by 5  $\mu$ mol/L AA either in control conditions (black line) or in cells pretreated for 10 min with 20  $\mu$ mol/L PKI (gray line).

**Table 1.** Statistics of responsive B-TECs in terms of intracellular calcium increase (probe FURA-2 AM) in different experiment conditions

Treatment	% Responsive cells ( $Ca_c$ increase)
AA	100
AA + PKI	1
AA + L-NAME	98
AA + PTIO	89
L-Arg	100
SNP	58
SNP + PKI	16
SNP (free $Ca_{out}$ )	0
SNAP	64
SNAP (free $Ca_{out}$ )	0
Forskolin	98
Forskolin (free $Ca_{out}$ )	77
Forskolin + L-NAME	6
Forskolin + PKI	2

NOTE: For further details, please see Results section.

NaF. Cells were centrifuged for 15 minutes at  $1,000 \times g$  and resuspended in lysis buffer containing 100 mmol/L Tris-HCl (pH 8.0), 1 mmol/L  $MgCl_2$  in the presence of protease inhibitors and frozen at  $-80^\circ C$  for at least 2 hours before use. Cells were subjected to one freeze-thaw cycle in the lysis buffer mixed with 2 $\times$  sucrose solution to give a final concentration of 250 mmol/L sucrose and then homogenized by passing through a syringe tip. Protein concentration was determined using the Quanti-iT protein assay (Invitrogen) following the manufacturer's instructions.

Conditions for SDS-PAGE and Western blotting were as described previously (27). Polyvinylidene difluoride membranes were blocked and incubated for 1 hour with rabbit IgG anti-eNOS phosphorylated at Ser<sup>1179</sup> of the bovine eNOS (corresponding to human Ser<sup>1177</sup>) antibody (Zymed, Invitrogen). The membrane was washed with TBS containing 0.1% Tween 20, incubated as required with horseradish peroxidase-conjugated antimouse IgG antibody or horseradish peroxidase-conjugated anti-rabbit IgG antibody (Amersham), washed, treated with SuperSignal West Pico chemiluminescent substrate (Pierce), and exposed to Amersham Hyperfilms (GE Healthcare). Results were obtained from at least three independent experiments.

### Data analysis and statistics

Images obtained from DAR4M-AM confocal measurements were analyzed with ImageJ, a public domain Java image processing software tool [Rasband W. ImageJ (imaging software). Version 1.32. NIH; 2004]. For each image sequence, regions of interest corresponding to single cells were selected, and the mean fluorescence intensity of each region of interest was computed.

For fura-2-AM ratiometric measurements, single cells were selected for each image sequence with Metafluor software (Universal Imaging). Cytosolic free calcium concentration ( $Ca_c$ ) was expressed as a ratio of emitted fluorescence ( $\lambda = 510$  nm) in correspondence to excitation wavelengths of 340 and 380 nm.

Igor software was used to further analyze both DAR4M-AM and fura-2-AM measurements. In particular, we considered the agonist-induced slope change as a quantitative criterion to distinguish a response to an agonist from noise.

One-way ANOVA was done to analyze the data sets. Post hoc tests were used to determine statistically significant differences among the groups (Student-Newman-Keuls test). The level of significance was  $P < 0.05$ .

Statistical analysis of wound healing assays was done using the Wilcoxon-Mann-Whitney test; the level of significance was set at  $P < 0.05$ .

## Results

### PKA is required for AA-induced calcium entry in B-TECs

Pretreatment of B-TECs with the membrane-permeable PKA inhibitory peptide myristoylated PKI<sub>14-22</sub> (10 minutes, 20  $\mu$ mol/L) completely abolished AA-induced calcium entry in 99% of the cells tested ( $n = 84$ ; Fig. 1; Table 1), suggesting a critical role of endogenous PKA in the activation of calcium signals by AA. The response to AA was also entirely prevented in 93% of the cells by pretreatment with staurosporine (10 minutes, 100 nmol/L;  $n = 79$ ), a less specific blocker of serine/threonine protein kinases.

### AA promotes B-TEC motility through PKA

The ability of AA to trigger B-TEC motility was tested using two different techniques: Boyden chamber assay and wound healing assay. We used Boyden's chamber in which

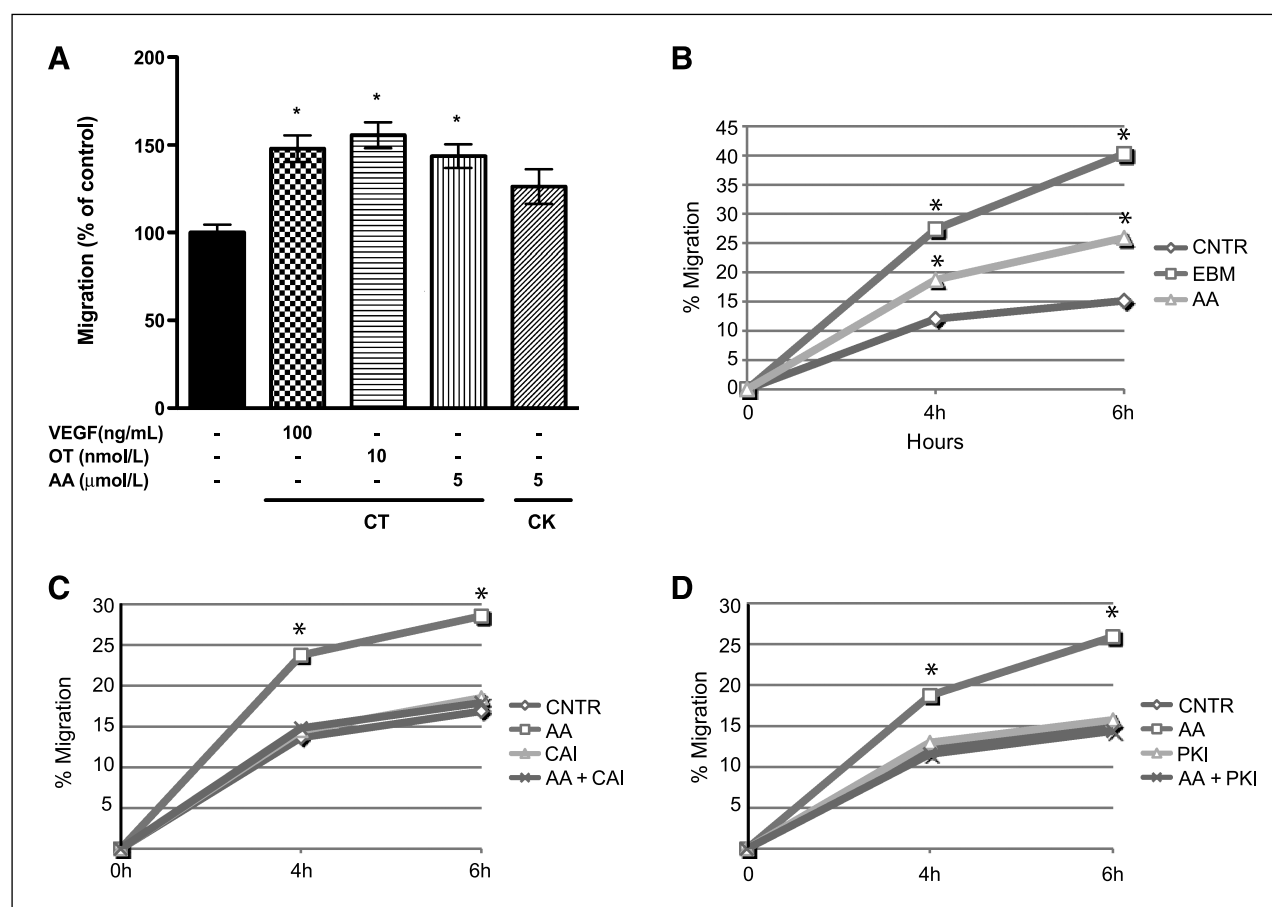


**FIGURE 2.** AA promotes motility and chemotaxis in B-TECs. A, chemotactic and chemokinetic response of B-TECs to AA (5  $\mu$ mol/L). The assay was done using a Boyden's chamber assay. VEGF (100 ng/mL) and oxytocin (OT; 10 nmol/L) were used as positive controls. Columns, mean of 9 to 23 replicates from 2 to 4 experiments; bars, SEM. \*,  $P < 0.05$ , compared with controls (ANOVA). CT, chemotaxis; CK, chemokinesis. B, time course (4-6 h) of a representative wound healing assay in different conditions: DMEM-0% FCS (CNTR); EBM-10% FCS (EBM); and DMEM-0% FCS + 5  $\mu$ mol/L AA (AA). C, time course (4-6 h) of a representative wound healing assay in different conditions: DMEM-0% FCS (CNTR); DMEM-0% FCS + 1  $\mu$ mol/L CAI (CAI); and DMEM-0% FCS + 5  $\mu$ mol/L AA + 1  $\mu$ mol/L CAI (AA + CAI). D, time course (4-6 h) of a representative wound healing assay in different conditions: DMEM-0% FCS (CNTR); DMEM-0% FCS + 20  $\mu$ mol/L PKI (PKI); and DMEM-0% FCS + 5  $\mu$ mol/L AA + 20  $\mu$ mol/L PKI (AA + PKI). \*,  $P < 0.05$ , compared with controls (Wilcoxon-Mann-Whitney test).

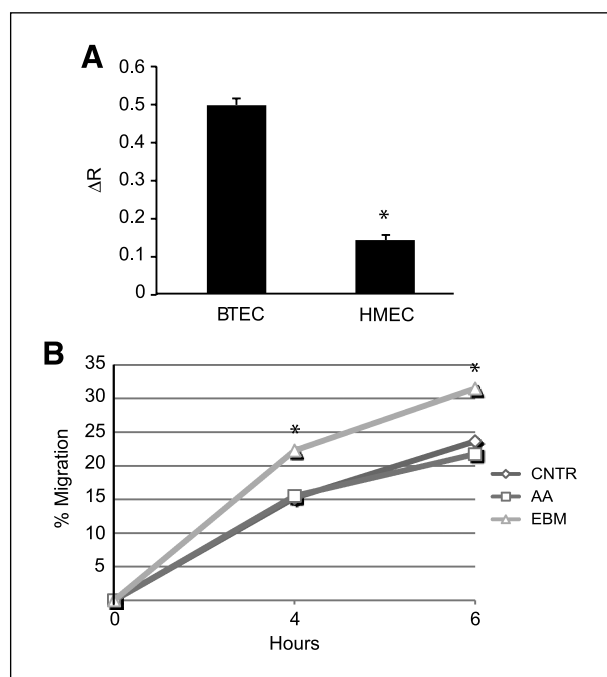


**FIGURE 3.** Comparison between the effects of AA on B-TECs and HMECs. A, statistics of peak amplitude (columns, mean; bars, SEM) of  $Ca_c$  signals activated by 5  $\mu\text{mol/L}$  AA in B-TECs and HMECs. \*,  $P < 0.05$ , compared with controls (ANOVA). B, time course (4–6 h) of a representative wound healing assay in different conditions in HMEC: DMEM-2% FCS (CNTR); EBM-10% FCS (EBM); and DMEM-2% FCS + 5  $\mu\text{mol/L}$  AA (AA). \*,  $P < 0.05$ , compared with controls (Wilcoxon-Mann-Whitney test).

chemoattraction or chemokinesis was assayed according to the placement of AA (Fig. 2A). When 5  $\mu\text{mol/L}$  AA was present both in the upper and lower chambers, chemokinesis was observed, although not significant compared with control. On the other hand, when AA was present only in the lower chamber, a significant migratory effect was detected. As a positive control, we used 100 ng/mL VEGF or 10 nmol/L oxytocin (12).

Moreover, we tested the ability of AA to increase B-TEC wound healing in a monolayer. Stimulation of wounded B-TEC monolayer with AA (4–6 hours; 5  $\mu\text{mol/L}$ ) induced a significant reduction of wound compared with the control condition (DMEM-0% FCS). As a positive control, wound healing was measured on B-TECs growing in EBM-10% FCS (Fig. 2B).

Preincubation of B-TECs with the antiangiogenic compound carboxyamidotriazole (CAI; 1  $\mu\text{mol/L}$ ), a well-known inhibitor of agonist-activated calcium channels, completely abolished AA-induced wound healing, clearly suggesting that calcium signals are required for this effect (Fig. 2C).

Having shown that AA-triggered  $Ca_c$  signals are PKA sensitive, we tested the effect of PKI on AA-dependent wound healing. Preincubation with PKI (10 minutes, 20  $\mu\text{mol/L}$ ) significantly reduced B-TEC motility specif-

ically promoted by AA, whereas no significant effect was observed in control conditions (Fig. 2D).

### AA fails to promote motility in normal human ECs

AA-dependent calcium signaling was less pronounced in normal HMECs compared with B-TECs (92% responsive cells;  $n = 26$ ; Fig. 3A). Notably, 5  $\mu\text{mol/L}$  AA failed to enhance HMEC motility in wound healing assays (Fig. 3B).

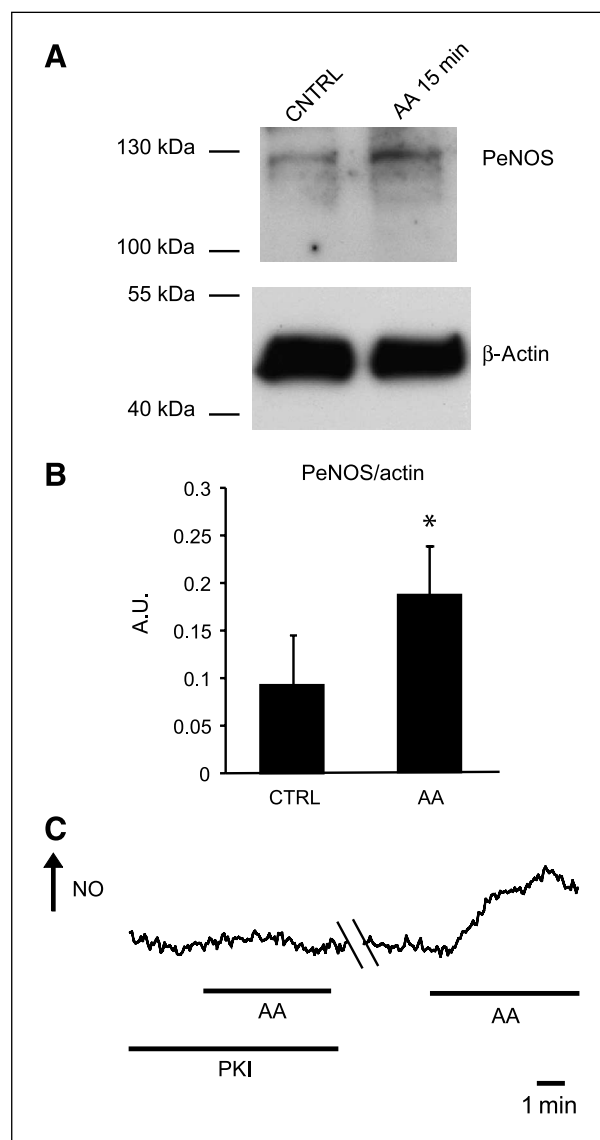


**FIGURE 4.** AA phosphorylates and activates eNOS in B-TECs.

A, Western blot showing eNOS phosphorylation and  $\beta$ -actin expression after 15 min of treatment with 5  $\mu\text{mol/L}$  AA. Representative of six experiments. B, quantification of AA-induced eNOS phosphorylation (columns, mean; bars, SEM). C, representative experiment showing NO measurement in single cells loaded with the NO-sensitive fluorescent probe DAR4M-AM. PKI-pretreated cells failed to respond to stimulation with 5  $\mu\text{mol/L}$  AA. After a prolonged wash in PKI-free tyrode solution (more than 5 min), the response to AA was restored.

**Table 2.** Statistics of responsive B-TECs in terms of intracellular NO increase (probe DAR-4M AM) in different experiment conditions

Treatment	% Responsive cells (NO increase)
AA	79
AA + PKI	30
Forskolin	76
Forskolin (free Ca <sub>out</sub> )	92

NOTE: For further details, please see Results section.

**AA promotes eNOS phosphorylation and activation in B-TECs**

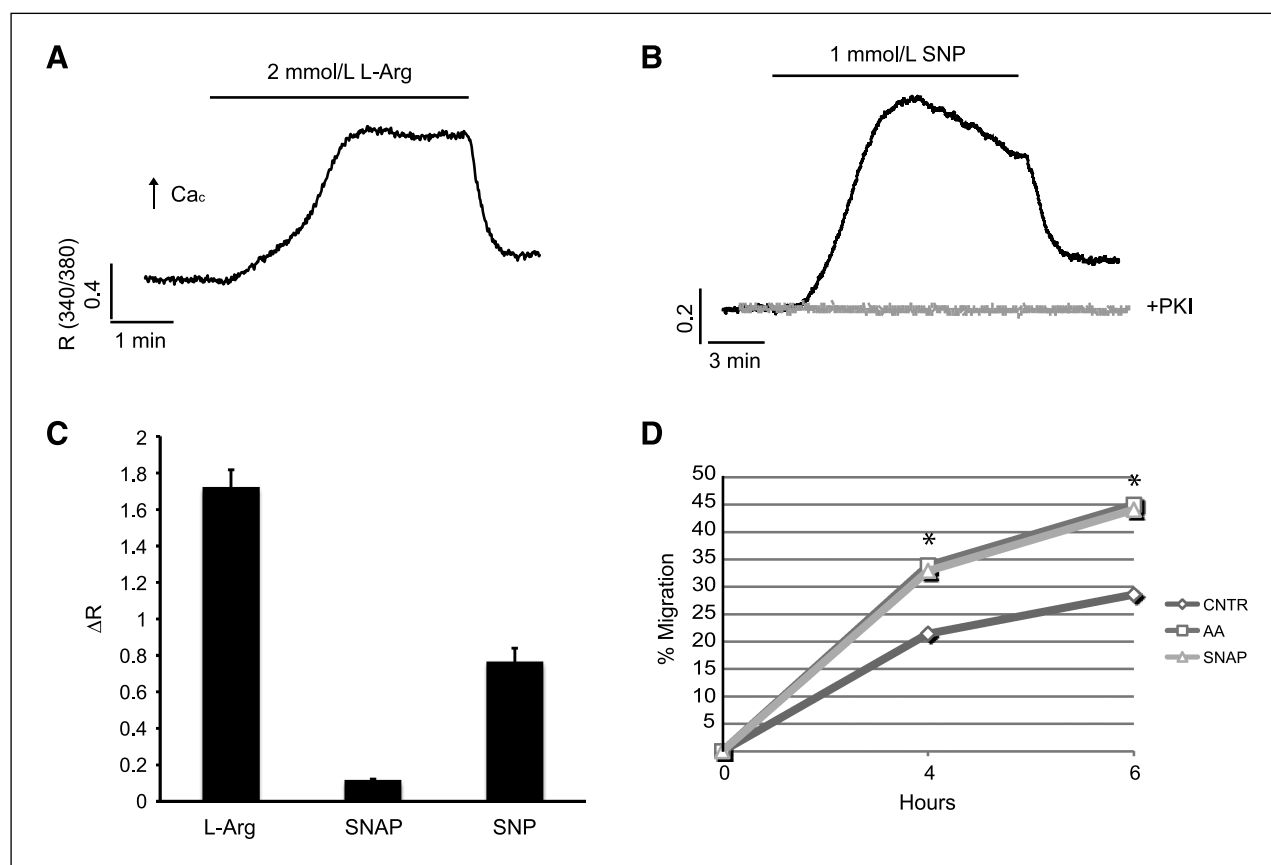
Because it is well known that serine/threonine phosphorylation is one of the regulatory mechanisms for eNOS activity, we performed Western blot experiments to test the ability of AA to promote eNOS phosphorylation in B-TECs. In particular, we used an antibody recognizing

human eNOS on Ser<sup>1177</sup>, a target for PKA phosphorylation (21). Treatment with AA (15 minutes, 5  $\mu$ mol/L) induced a significant eNOS phosphorylation compared with control conditions (Fig. 4A and B).

Even if eNOS phosphorylation is required for its activity, it may not be sufficient to activate the enzyme. For this reason, we tested the ability of AA to increase intracellular NO levels using the NO-sensitive fluorescent dye DAR4M-AM. Acute stimulation with 5  $\mu$ mol/L AA increased intracellular NO in 79% of the cell tested ( $n = 68$ ). Pretreatment with PKI (10 minutes, 20  $\mu$ mol/L) completely prevented the response to AA in 70% of the cells ( $n = 104$ ). The inhibitory effect was reversible, as shown by the recovery of AA-induced NO increase after intense and prolonged wash (more than 5 minutes) in 82% of the cells ( $n = 45$ ; Fig. 4C; Table 2).

**NO triggers calcium entry and B-TEC migration**

Several groups, including ours, reported the ability of NO to open calcium channels in the plasma membrane of ECs (6, 28). For these reasons, we investigated the

**FIGURE 5.** Calcium entry activated by NO in B-TECs. A and B, representative experiments showing Ca<sub>c</sub> signals activated by 2 mmol/L L-Arg (A) or 1 mmol/L SNP (B) in single cells. Dotted trace in B shows representative cells preincubated with PKI (10 min, 20  $\mu$ mol/L) and stimulated with 1 mmol/L SNP.

C, peak amplitude (columns, mean; bars, SEM) of Ca<sub>c</sub> signals activated by 2 mmol/L L-Arg, 10  $\mu$ mol/L SNAP, or 1 mmol/L SNP. \*,  $P < 0.05$ , compared with controls (ANOVA). D, time course (4-6 h) of a representative wound healing assay in different conditions: DMEM-0% FCS (CNTR); DMEM-0% FCS + 5  $\mu$ mol/L AA; and DMEM-0% FCS + 10  $\mu$ mol/L SNAP (SNAP). \*,  $P < 0.05$ , compared with controls (Wilcoxon-Mann-Whitney test).

effects of NO on  $Ca_c$  signaling in B-TECs. These were assessed either indirectly by the use of L-Arg (eNOS substrate and activator, which enters the cell through a specific membrane carrier) or directly with sodium nitroprusside (SNP) and *S*-nitroso-*N*-acetylpenicillamine (SNAP), two NO donors. Acute application of 2 mmol/L L-Arg induced a large calcium increase (100% responsive cells;  $n = 53$ ; Fig. 5A and C; Table 1). Consistently, also stimulation with either 1 mmol/L SNP (58% responsive cells,  $n = 80$ ; Fig. 5B and C; Table 1) or 10  $\mu$ mol/L SNAP (64% responsive cells,  $n = 45$ ; Fig. 5C; Table 1) evoked calcium signals, which were completely abolished in calcium-free external solution (0% responsive cells for both the donors;  $n = 19$ ; Table 1). Preincubation with PKI (10 minutes, 20  $\mu$ mol/L) completely abolished the response to SNP in 84% of the cells ( $n = 38$ ; Fig. 5B; Table 1). When B-TECs were treated with 10  $\mu$ mol/L SNAP, their motility was enhanced, as shown by wound healing assay (Fig. 5D).

#### NO release is involved in AA-mediated calcium entry in B-TECs

$Ca_c$  signals triggered by AA were significantly affected by pretreatment with  $N^G$ -nitro-L-arginine methyl ester (L-NAME; 10 minutes, 5 mmol/L; 100% responsive cells,  $n = 47$ ; Fig. 6A; Table 1). Consistently, the response to AA was significantly altered by pretreatment with the NO scavenger 2-phenyl-4,4,5,5-tetramethylimidazole-1-oxyl 3-oxide (PTIO; 10 minutes, 1 mmol/L; 89% responsive cells,  $n = 61$ ; Fig. 6A; Table 1).

#### NO release is required for AA-mediated B-TEC migration

To evaluate the functional role of NO as a mediator of B-TEC motility induced by AA, we performed wound healing assays in cells pretreated either with L-NAME (5 mmol/L) or with PTIO (100  $\mu$ mol/L). In both conditions, AA-induced wound healing was completely prevented (Fig. 6B and C).

#### The cAMP/PKA pathway triggers NO release and calcium entry independently of AA release

Because many agonists promote cAMP increase in ECs, we investigated the effects of a simple cAMP increase (leading to PKA activation) in the absence of AA stimulation. Acute application with 10  $\mu$ mol/L forskolin enhanced intracellular NO release in 76% of B-TECs ( $n = 34$ ). This effect was not due to a cAMP-dependent calcium entry because stimulation with forskolin in calcium-free extracellular solution was still able to increase NO levels (92% responsive cells,  $n = 40$ ; Fig. 7A; Table 2).

Acute treatment with 10  $\mu$ mol/L forskolin increased  $Ca_c$  levels (98% responsive cells,  $n = 60$ ; Fig. 7B and C; Table 1). Only a small  $Ca_c$  response was detectable in calcium-free external solution in 77% of the cells tested ( $n = 49$ ), suggesting a little contribution from intracellular calcium

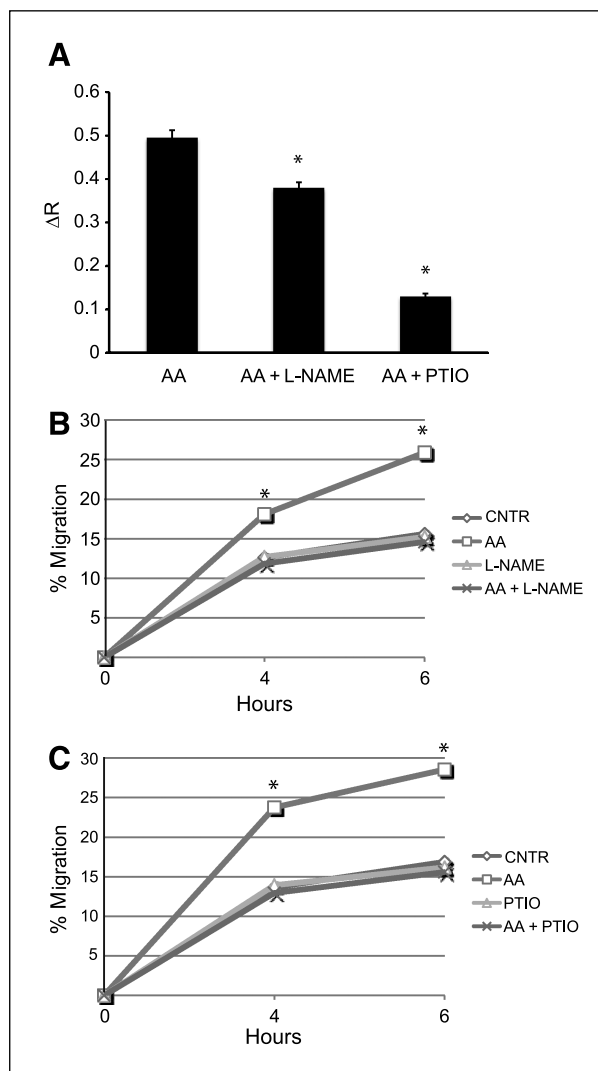


**FIGURE 6.** NO mediates AA-dependent calcium signals and motility in B-TECs. A, statistics of peak amplitude (columns, mean; bars, SEM) of  $Ca_c$  signals activated by 5  $\mu$ mol/L AA in control cells (AA) or in cells preincubated for 10 min with either 5 mmol/L L-NAME or 1 mmol/L PTIO. \*,  $P < 0.05$ , compared with controls (ANOVA). B, time course (4–6 h) of a representative wound healing assay in different conditions: DMEM-0% FCS (CNTR); DMEM-0% FCS + 5  $\mu$ mol/L AA (AA); DMEM-0% FCS + 5 mmol/L L-NAME; and DMEM-0% FCS + 5  $\mu$ mol/L AA + 5 mmol/L L-NAME. C, time course (4–6 h) of a representative wound healing assay in different conditions: DMEM-0% FCS (CNTR); DMEM-0% FCS + 5  $\mu$ mol/L AA (AA); DMEM-0% FCS + 100  $\mu$ mol/L PTIO; and DMEM-0% FCS + 5  $\mu$ mol/L AA + 100  $\mu$ mol/L PTIO. \*,  $P < 0.05$ , compared with controls (Wilcoxon-Mann-Whitney test).

stores (dotted line in Fig. 7B and C; Table 1). Preincubation with 5 mmol/L L-NAME (10 minutes) completely abolished the response to forskolin in 94% of the cells ( $n = 67$ ; Table 1), showing an involvement of NOS in cAMP-dependent  $Ca_c$  signals.

Interestingly, also pretreatment with PKI (10 minutes, 20  $\mu$ mol/L) completely abolished the  $Ca_c$  increase stimulated by forskolin in 98% of the cells ( $n = 40$ ; Table 1),

providing evidence for a key role of PKA activation rather than cAMP-gated channels.

## Discussion

The main goal of this work is to investigate the regulatory mechanisms of previously described AA-activated

proangiogenic calcium entry in B-TECs. In B-TECs, low concentrations of AA activate a store-independent calcium entry with similar properties previously observed in BAECs. This event is involved in tubulogenesis progression and is downregulated in the later phases of tubule formation (5, 29). Here, we show that the cAMP/PKA pathway is involved in AA-induced  $\text{Ca}^{2+}$  entry. B-TEC pretreatment with PKA inhibitory peptide, PKI, completely abolished AA-induced calcium entry, showing that PKA is necessary for  $\text{Ca}_c$  signals triggered by the fatty acid (Fig. 1).

As indicated by wound healing and Boyden chamber assays, AA at low concentrations is motogenic and chemoattractive for B-TECs (see Fig. 2A and B). Notably, the dramatic effect of the antiangiogenic compound CAI, an agonist-activated calcium entry inhibitor, reveals that AA-induced wound healing is dependent on calcium signals (Fig. 2C). These data are in agreement with the previously described calcium-dependent tubulogenic action of the fatty acid (5). AA-induced wound healing is also abolished by PKI preincubation, providing a functional link between the cAMP/PKA pathways described above and the biological activities of the fatty acid (Fig. 2D).

The observation that normal HMECs are less responsive than B-TECs to stimulation with AA in terms of calcium increase (Fig. 3A) and entirely unaffected by the fatty acid in cell motility (Fig. 3B) is very intriguing for its potential biomedical application and could help to develop a more selective pharmacologic approach to tumor angiogenesis. The simplest explanation could be that calcium increase activated by AA in normal ECs is too low in extent to trigger the same functional effects as in B-TECs. Nevertheless, other factors responsible for this difference could be the spatiotemporal dynamics of calcium signals and the type of channels involved (see also below). This point, far beyond the aim of this work, deserves to be investigated in more detail in the future.

Because NOS are modulated by PKA-dependent phosphorylation and we previously reported the ability of AA to release NO in BAECs (6), we performed single-cell fluorimetric measurements using the NO-sensitive probe DAR4M-AM and confirmed that AA leads to NO release also in B-TECs (Fig. 4C). Furthermore, Western blot experiments suggest that this is likely due, at least in part, to eNOS phosphorylation in a serine residue target for PKA-dependent phosphorylation (Fig. 4A and B), even if we cannot exclude the involvement of other NOS isoforms (iNOS and nNOS) that could play a role in tumor angiogenesis (13, 30). NOS phosphorylation is functionally relevant because pretreatment with PKI leads to a complete inhibition of AA-induced NO release (Fig. 4C). The mechanism responsible for AA-induced PKA recruitment is unknown in these cells, but in rat aortic endothelium, cAMP increase is mediated by prostaglandin  $\text{I}_2$  through its G-protein-coupled membrane receptor (31).

Taken together, these data suggest that PKA could regulate AA-dependent  $\text{Ca}_c$  signals through at least two (possibly coexisting) pathways (Fig. 8): (a) phosphorylation and

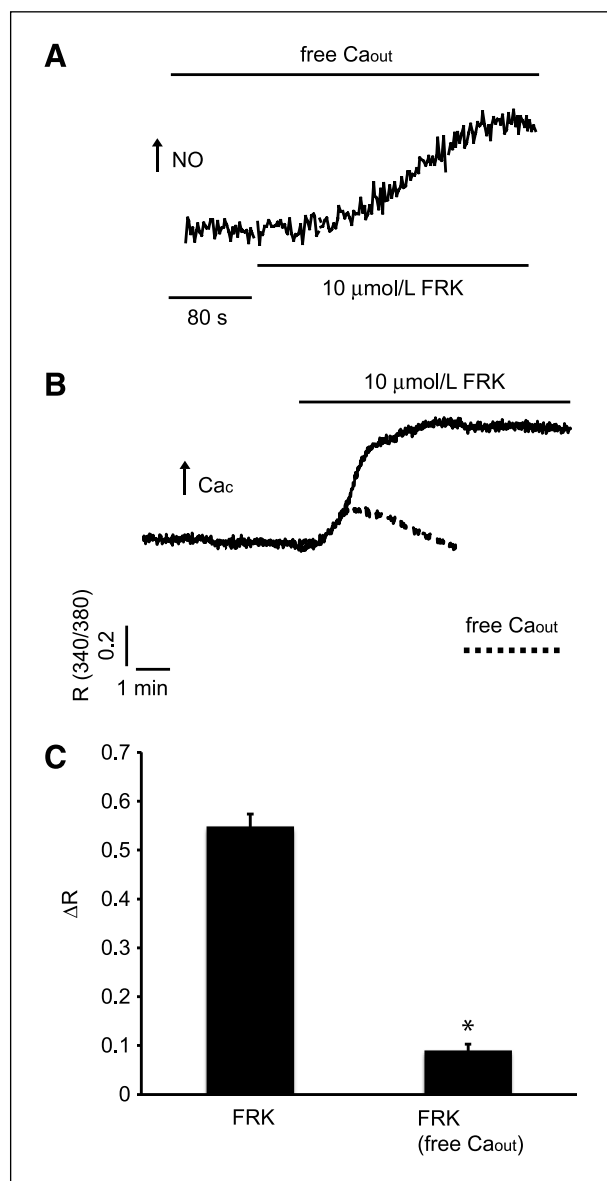


**FIGURE 7.** cAMP/PKA-dependent  $\text{Ca}_c$  signals in B-TECs. A, a representative experiment of NO measurement in single cells loaded with DAR4M-AM and acutely stimulated with 10  $\mu\text{mol/L}$  forskolin (FRK) in calcium-free external solution. B, a representative experiment showing  $\text{Ca}_c$  increase induced by 10  $\mu\text{mol/L}$  forskolin stimulation; dotted trace indicates a typical response to forskolin in calcium-free external solution. C, peak amplitude (columns, mean; bars, SEM) of  $\text{Ca}_c$  signals activated by acute stimulation with 10  $\mu\text{mol/L}$  forskolin either in control conditions (FRK) or in calcium-free external solution (FRK + free  $\text{Ca}_{\text{out}}$ ). \*,  $P < 0.05$ , compared with controls (ANOVA).

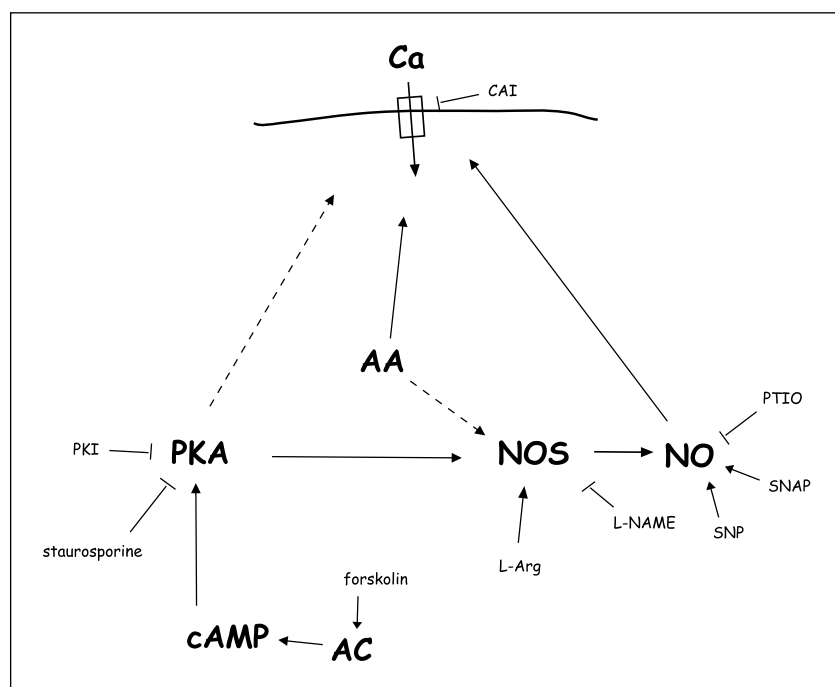


**FIGURE 8.** Schematic representation of the pathways described in this study. Calcium entry is represented as due to the opening of a single channel type only for graphical purpose (see Discussion). Dotted lines indicate indirect or not fully clarified processes. See text for details.

activation of eNOS and (b) direct and/or indirect phosphorylation of AA-activated channels. The first hypothesis, discussed previously, is supported by several reports on PKA-dependent NOS phosphorylation and activation (21, 32, 33). The second explanation, pointing to an effect on calcium channels, would be in agreement with PKA-dependent phosphorylation of calcium-permeable channels reported for ECs and other cell types (34-36).

Similarly to AA-dependent calcium entry, NO-activated calcium signals triggered by direct application of NO donors are significantly affected on pretreatment with PKI (Fig. 5B and C).

We do not know the identity of AA- and NO-activated channel(s) in B-TECs, although some candidates can be considered. TRPV1 and TRPV4 (both expressed in B-TEC)<sup>5</sup> are regulated by fatty acids, including AA, and their metabolites. They are also modulated by NO through S-nitrosylation and sensitized by PKA phosphorylation (37-40). TRPC3 and TRPC6 are activated by fatty acids and substrate for nitrosylation as well, and the cAMP/PKA pathway could enhance their insertion into the plasma membrane (34). Finally, in m3-HEK cell line, the so-called arachidonate-regulated channels require PKA phosphorylation and are composed of Orai1 and Orai3 proteins (35, 41).

B-TECs could express two (or more than two) types of calcium-permeable, PKA-dependent ion channels: one activated by AA and another by NO. Such hypothesis is in agreement with several previous observations on the prop-

erties of distinct AA- and NO-operated calcium channels in ECs (6, 28). Here, the picture seems particularly complex. In principle, AA, being able to recruit eNOS (and eventually other NOS isoforms) and to release NO, could open both channels. Unfortunately, NO-sensitive fluorescent probes are not quantitative and do not allow comparison of the extent of NO release by AA and NO donors. Nevertheless, we cannot exclude the existence of a single channel type underlying a double regulation. At low NO concentrations, AA might trigger channel opening; at higher NO concentrations, NO could act as the major activator even in the absence of AA. cAMP/PKA-dependent phosphorylation is a key regulatory mechanism acting both indirectly on eNOS activation and directly on AA- and NO-dependent calcium channel(s) or channel-associated proteins.

Interestingly, AA-dependent calcium signals were significantly smaller when B-TECs were pretreated with either a NOS inhibitor (L-NAME) or a NO scavenger (PTIO), but not were fully abolished (Table 1; Fig. 6A). This observation suggests the existence of a NO-independent component of AA-activated calcium entry, consistent with previous data reported by our group in BAECs (6). On the other hand, the same treatment entirely prevented AA-induced B-TEC motility, clearly indicating that NO is required for this effect (Fig. 6B and C). Accordingly, direct NO application by the NO donor SNAP enhanced B-TEC motility, mimicking the effect of AA (Fig. 5D).

The role of PKA is not only permissive on a AA-dependent pathway leading to calcium entry but is also relevant by itself. Indeed, direct stimulation of the cAMP/PKA pathway by acute forskolin application induced Ca<sub>c</sub> and NO increase in B-TECs (Fig. 7A and B). Only a

<sup>5</sup> Unpublished observations.

small  $Ca_c$  increase was detectable in calcium-free external solution, indicating a little contribution from intracellular calcium stores (dotted line in Fig. 7B; Table 1). The ability of PKI to abolish calcium increase triggered by forskolin indicates that the effect is entirely due to PKA activation and not to a recruitment of cAMP-gated channels (Table 1). From these results, we can argue that agonists that increase cAMP levels in ECs, even without affecting AA release, are expected to facilitate the following calcium entry promoted by AA-releasing proangiogenic stimuli.

Remarkably, calcium signals evoked by forskolin were almost completely inhibited by the NOS inhibitor L-NAME (Table 1). This evidence suggests that PKA-dependent calcium entry is entirely due to the NOS/NO pathway, differently from AA-induced calcium response, only in part sensitive to L-NAME (Fig. 6A; Table 1). This observation is in agreement with a recent report on proangiogenic activity triggered by forskolin through the PI3K, Akt, eNOS pathways in human umbilical vascular ECs (22). The ability of L-NAME to exert a near-complete abolishment of forskolin-triggered calcium entry leads us also to confirm that the PKA-dependent phosphorylation of AA-activated calcium channels probably acts in a permissive way, but it is not activatory by itself (i.e., in the absence of AA).

In conclusion, here we show for the first time that the cAMP/PKA pathway regulates proangiogenic calcium entry and is required for motility in breast cancer-derived human ECs but not in ECs from normal tissues. The peculiar behavior of B-TECs reported here supports the idea that tumor-derived ECs are a more suitable model to evaluate the clinical potential of antiangiogenic and anti-tumor agents.

### Disclosure of Potential Conflicts of Interest

No potential conflicts of interest were disclosed.

### Acknowledgments

We thank Prof. Benedetta Bussolati (MBC, Torino, Italy) for kindly providing B-TECs.

### Grant Support

The University of Torino, Regione Piemonte (Ricerca Scientifica Applicata Sanita). The costs of publication of this article were defrayed in part by the payment of page charges. This article must therefore be hereby marked *advertisement* in accordance with 18 U.S.C. Section 1734 solely to indicate this fact.

Received 01/04/2010; revised 08/16/2010; accepted 09/13/2010; published OnlineFirst 09/24/2010.

### References

- Munaron L. Intracellular calcium, endothelial cells and angiogenesis. *Recent Patents Anticancer Drug Discov* 2006;1:105–19.
- Munaron L, Tomatis C, Pla AF. The secret marriage between calcium and tumor angiogenesis. *Technol Cancer Res Treat* 2008;7:335–9.
- Munaron L, Antoniotti S, Lovisolio D. Intracellular calcium signals and control of cell proliferation: how many mechanisms? *J Cell Mol Med* 2004;8:161–8.
- Munaron L, Pla AF. Endothelial calcium machinery and angiogenesis: understanding physiology to interfere with pathology. *Curr Med Chem* 2009;16:4691–703.
- Fiorio Pla A, Grange C, Antoniotti S, et al. Arachidonic acid-induced  $Ca^{2+}$  entry is involved in early steps of tumor angiogenesis. *Mol Cancer Res* 2008;6:535–45.
- Mottola A, Antoniotti S, Lovisolio D, Munaron L. Regulation of non-capacitative calcium entry by arachidonic acid and nitric oxide in endothelial cells. *FASEB J* 2005;19:2075–7.
- Tomatis C, Fiorio Pla A, Munaron L. Cytosolic calcium microdomains by arachidonic acid and nitric oxide in endothelial cells. *Cell Calcium* 2007;41:261–9.
- Carmeliet P. VEGF as a key mediator of angiogenesis in cancer. *Oncology* 2005;69 Suppl 3:4–10.
- Bussolati B, Deambrosio I, Russo S, Deregibus MC, Camussi G. Altered angiogenesis and survival in human tumor-derived endothelial cells. *FASEB J* 2003;17:1159–61.
- Grange C, Bussolati B, Bruno S, Fonsato V, Sapino A, Camussi G. Isolation and characterization of human breast tumor-derived endothelial cells. *Oncol Rep* 2006;15:381–6.
- Baluk P, Morikawa S, Haskell A, Mancuso M, McDonald DM. Abnormalities of basement membrane on blood vessels and endothelial sprouts in tumors. *Am J Pathol* 2003;163:1801–15.
- Cassoni P, Marrocco T, Bussolati B, et al. Oxytocin induces proliferation and migration in immortalized human dermal microvascular endothelial cells and human breast tumor-derived endothelial cells. *Mol Cancer Res* 2006;4:351–9.
- Fukumura D, Kashiwagi S, Jain RK. The role of nitric oxide in tumour progression. *Nat Rev Cancer* 2006;6:521–34.
- Ziche M, Morbidelli L. Nitric oxide and angiogenesis. *J Neurooncol* 2000;50:139–48.
- Berkels R, Suerhoff S, Roesen R, Klaus W. Nitric oxide causes a cGMP-independent intracellular calcium rise in porcine endothelial cells—a paradox? *Microvasc Res* 2000;59:38–44.
- Cooke JP, Losordo DW. Nitric oxide and angiogenesis. *Circulation* 2002;105:2133–5.
- Dedkova EN, Blatter LA. Nitric oxide inhibits capacitative  $Ca^{2+}$  entry and enhances endoplasmic reticulum  $Ca^{2+}$  uptake in bovine vascular endothelial cells. *J Physiol (Lond)* 2002;539:77–91.
- Dimmeler S, Dernbach E, Zeiher AM. Phosphorylation of the endothelial nitric oxide synthase at ser-1177 is required for VEGF-induced endothelial cell migration. *FEBS Lett* 2000;477:258–62.
- Pepine CJ. The impact of nitric oxide in cardiovascular medicine: untapped potential utility. *Am J Med* 2009;122:S10–5.
- Yao X, Huang Y. From nitric oxide to endothelial cytosolic  $Ca^{2+}$ : a negative feedback control. *Trends Pharmacol Sci* 2003;24:263–6.
- Butt E, Bernhardt M, Smolenski A, et al. Endothelial nitric-oxide synthase (type III) is activated and becomes calcium independent upon phosphorylation by cyclic nucleotide-dependent protein kinases. *J Biol Chem* 2000;275:5179–87.
- Namkoong S, Kim CK, Cho YL, et al. Forskolin increases angiogenesis through the coordinated cross-talk of PKA-dependent VEGF expression and Epac-mediated PI3K/Akt/eNOS signaling. *Cell Signal* 2009;21:906–15.
- Kwan HY, Huang Y, Yao X. TRP channels in endothelial function and dysfunction. *Biochim Biophys Acta* 2007;1772:907–14.
- Kwan HY, Huang Y, Yao XQ, Leung FP. Role of cyclic nucleotides in the control of cytosolic Ca levels in vascular endothelial cells. *Clin Exp Pharmacol Physiol* 2009;36:857–66.
- Yao X, Garland CJ. Recent developments in vascular endothelial cell transient receptor potential channels. *Circ Res* 2005;97:853–63.
- Yao X, Kwan HY, Huang Y. Regulation of TRP channels by phosphorylation. *Neurosignals* 2005;14:273–80.
- Fiorio Pla A, Maric D, Brazer SC, et al. Canonical transient receptor potential 1 plays a role in basic fibroblast growth factor (bFGF)/FGF

- receptor-1-induced  $\text{Ca}^{2+}$  entry and embryonic rat neural stem cell proliferation. *J Neurosci* 2005;25:2687–701.
28. Yao XQ, Huang Y. From nitric oxide to endothelial cytosolic  $\text{Ca}^{2+}$ : a negative feedback control. *Trends Pharmacol Sci* 2003;24:263–6.
  29. Fiorio Pla A, Munaron L. Calcium influx, arachidonic acid and control of endothelial cell proliferation. *Cell Calcium* 2001;30:235–44.
  30. Seidel B, Stanarius A, Wolf G. Differential expression of neuronal and endothelial nitric oxide synthase in blood vessels of the rat brain. *Neurosci Lett* 1997;239:109–12.
  31. Ray C. The cellular mechanisms by which adenosine evokes release of nitric oxide from rat aortic endothelium. *J Physiol (Lond)* 2005;570:85–96.
  32. Cokic VP, Beleslin-Cokic BB, Tomic M, Stojilkovic SS, Noguchi CT, Schechter AN. Hydroxyurea induces the eNOS-cGMP pathway in endothelial cells. *Blood* 2006;108:184–91.
  33. Hashimoto A, Miyakoda G, Hirose Y, Mori T. Activation of endothelial nitric oxide synthase by cilostazol via a cAMP/protein kinase A- and phosphatidylinositol 3-kinase/Akt-dependent mechanism. *Atherosclerosis* 2006;189:350–7.
  34. Fleming I, Rueben A, Popp R, et al. Epoxyeicosatrienoic acids regulate Trp channel dependent  $\text{Ca}^{2+}$  signaling and hyperpolarization in endothelial cells. *Arterioscler Thromb Vasc Biol* 2007;27:2612–8.
  35. Mignen O, Thompson JL, Shuttleworth TJ. Arachidonate-regulated  $\text{Ca}^{2+}$ -selective (ARC) channel activity is modulated by phosphorylation and involves an A-kinase anchoring protein. *J Physiol* 2005;567:787–98.
  36. Zhang X, Li L, McNaughton PA. Proinflammatory mediators modulate the heat-activated ion channel TRPV1 via the scaffolding protein AKAP79/150. *Neuron* 2008;59:450–61.
  37. Peng H, Lewandrowski U, Müller B, Sickmann A, Walz G, Wegierski T. Identification of a Protein Kinase C-dependent phosphorylation site involved in sensitization of TRPV4 channel. *Biochem Biophys Res Commun* 2019;391:1721–5.
  38. Yoshida T, Inoue R, Morii T, et al. Nitric oxide activates TRP channels by cysteine S-nitrosylation. *Nat Chem Biol* 2006;2:596–607.
  39. Jeske NA, Diogenes A, Ruparel NB, et al. A-kinase anchoring protein mediates TRPV1 thermal hyperalgesia through PKA phosphorylation of TRPV1. *Pain* 2008;138:604–16.
  40. Schnizler K, Shutov LP, Van Kanegan MJ, et al. Protein kinase A anchoring via AKAP150 is essential for TRPV1 modulation by forskolin and prostaglandin E2 in mouse sensory neurons. *J Neurosci* 2008;28:4904–17.
  41. Mignen O, Thompson JL, Shuttleworth TJ. Both Orai1 and Orai3 are essential components of the arachidonate-regulated  $\text{Ca}^{2+}$ -selective (ARC) channels. *J Physiol (Lond)* 2008;586:185–95.

# Molecular Cancer Research

## Multiple Roles of Protein Kinase A in Arachidonic Acid–Mediated Ca<sup>2+</sup> Entry and Tumor-Derived Human Endothelial Cell Migration

Alessandra Fiorio Pla, Tullio Genova, Emanuela Pupo, et al.

*Mol Cancer Res* 2010;8:1466-1476. Published OnlineFirst September 24, 2010.

**Updated version** Access the most recent version of this article at:  
doi:[10.1158/1541-7786.MCR-10-0002](https://doi.org/10.1158/1541-7786.MCR-10-0002)

**Cited articles** This article cites 40 articles, 9 of which you can access for free at:  
<http://mcr.aacrjournals.org/content/8/11/1466.full#ref-list-1>

**Citing articles** This article has been cited by 2 HighWire-hosted articles. Access the articles at:  
<http://mcr.aacrjournals.org/content/8/11/1466.full#related-urls>

**E-mail alerts** [Sign up to receive free email-alerts](#) related to this article or journal.

**Reprints and Subscriptions** To order reprints of this article or to subscribe to the journal, contact the AACR Publications Department at [pubs@aacr.org](mailto:pubs@aacr.org).

**Permissions** To request permission to re-use all or part of this article, use this link  
<http://mcr.aacrjournals.org/content/8/11/1466>.  
Click on "Request Permissions" which will take you to the Copyright Clearance Center's (CCC) Rightslink site.